

Supporting Information

***N,N'*-Dihydropentazapentacenes (DHTA) in thin film transistors**

Fabian Paulus,^a Benjamin D. Lindner,^a Hilmar Reiß,^a Frank Rominger,^a Andreas Leineweber,^b Yana Vaynzof,^{c,d} Henning Sirringhaus^e and Uwe H. F. Bunz^{a,d*}

^a F. Paulus, B. Lindner, H. Reiß, Dr. F. Rominger, Prof. U. Bunz, Institute for Organic Chemistry, Ruprecht-Karls-University of Heidelberg, Im Neuenheimer Feld 270, 69120 Heidelberg, Germany, uwe.bunz@oci.uni-heidelberg.de

^b Dr. A. Leineweber, Max Planck Institute for Intelligent Systems (formerly Max Planck Institute for Metals Research) Heisenbergstr. 3, 70569 Stuttgart, Germany
currently at: Institute of Materials Science, Technische Universität Bergakademie Freiberg, Gustav-Zeuner-Str. 5, 09599 Freiberg, Germany

^c Prof. Dr. Y. Vaynzof, Kirchoff-Institute for Physics, Ruprecht-Karls-University of Heidelberg Im Neuenheimer Feld 227, 69120 Heidelberg, Germany

^d Prof. Y. Vaynzof, Prof. U. Bunz, Centre for Advanced Materials, Ruprecht-Karls-University of Heidelberg Im Neuenheimer Feld 225, 69120 Heidelberg, Germany

^e Prof. H. Sirringhaus Cavendish Laboratory, J J Thomson Ave., University Cambridge Cambridge CB3 0HE, United Kingdom

Content:

- A) General Methods**
- B) Synthesis**
- C) Analytical Data DHTA-F₂**
- D) Optical properties of DHTA-compounds**
- E) Polarized optical microscopy of thin films**
- F) Electrical Characterization**
- G) XRD data**
- H) Summarised structural data**
- I) References**

- A) General Methods**

Synthetic work & characterisation:

All reagents and solvents were obtained from Fisher Scientific, ABCR, Alfa Aesar, Sigma-Aldrich or VWR and were used without further purification. All of the other absolute solvents were dried by a MB SPS-800 using drying columns. Preparation of air- and moisture-sensitive materials was carried out in oven dried flasks under an atmosphere of argon using Schlenk-techniques. Flash column chromatography was performed on silica gel from Macherey, Nagel & Co. KG, Düren

(Germany) (particle size: 0.04-0.063 mm). Melting points were determined with a Melting Point Apparatus MEL-TEMP (Electrothermal, Rochford, UK) and are uncorrected.

¹H-NMR, ¹³C-NMR and ¹⁹F-NMR spectra were recorded at room temperature on Bruker Avance DRX 300 (300 MHz), Bruker Avance III 300 (300 MHz), Bruker Avance III 400 (400 MHz), Bruker Avance III 500 (500 MHz) and Bruker Avance III 600 (600 MHz). Chemical shifts (δ) are reported in parts per million (ppm) relative to residual undeuterated solvent peak.¹ The following abbreviations are used to indicate the signal multiplicity: s (singlet), d (doublet), t (triplet), q (quartet), m (multiplet), dd (doublet of doublet), bs (broad singlet). All **NMR spectra** were integrated and processed using MestReC 4.7. **Infrared (IR) spectra** were recorded on a Jasco FT/IR-4100 spectrometer. **Absorption spectra** were recorded on a Jasco UV-VIS V-670 for measurements in solution. Thin films were spin coated on spectroil substrates, annealed at 80 °C and measured using a UV-Vis Hewlett-Packard spectrometer. **Emission spectra** were recorded on a Jasco FP-6500. **Elemental Analysis** was performed by the Microanalytical Laboratory of the University of Heidelberg using an Elementar Vario EL machine. **MS spectra** were recorded on a Vakuu Generators ZAB-2F, Finnigan MAT TSQ 700 or JEOL JMS-700 spectrometer.

Film preparation: All organic semiconductors were deposited on a cross-linked polyimide film (ca 40nm thick) on 1737F glass samples (PGO, Iserlohn, Germany) following the procedure from Sakanoue *et al.*² Polyimide films were used to provide a good wettability of all organic solvents and solutions on the substrate and support a good film formation and crystallisation. If untreated glass is used the organic films are not continuous and most often inhomogeneous. The organic semiconductors were spin cast from various solutions in a nitrogen purged glovebox and dried at 80 °C on a hotplate. The average film thicknesses were between 30-40 nm. Layer thicknesses were determined by a stylus profiler (DektakXT, Bruker).

Cross-polarised optical microscopy (POM): thin films were spin coated on polyimide coated glass substrates and optical images were taken using a Nikon Eclipse LV100POL microscope. Films for POM were prepared on polyimide coated glass substrates prepared in identical fashion to those prepared for device fabrication.

Ultra-Violet photoemission spectroscopy (UPS): Thin films of **DHTA-X₂** were spin coated on Au (50nm)/Si substrates. The samples were then transferred into the ultrahigh vacuum (UHV) chamber (ESCALAB 250Xi) for UPS measurements. The measurements were performed using a double-differentially pumped He gas ($h\nu = 21.22$ eV) with a pass energy of 2 eV.

Atomic Force Microscopy (AFM): AFM was performed in tapping mode using a Digital Instruments Nanoscope IIIa microscope. Films for AFM were prepared on polyimide coated glass substrates prepared in identical fashion to those prepared for device fabrication.

Device fabrication and characterisation: Bottom-contact top-gate transistors were fabricated on polyimide coated glass substrates (see above).² Gold source and drain electrodes (20 nm) were patterned by double layer resist photolithography. The electrodes were modified after lift-off with pentafluorobenzenethiol (PFBT) to enhance hole injection. Next, the substrates were transferred into a N₂ glovebox for all subsequent processing steps. The molecules were spin coated from a 20 mg/ml solution of various solvents at 1500rpm. The films were annealed at 80 °C for 30 minutes. A ca. 700 nm thick perfluorinated polymer CYTOP (Asahi Glass) was spin coated as dielectric layer and annealed at 90 °C for 30 min. CYTOP and therefore CYTOP-solvent (CT-180) was used as orthogonal solvent and prevents any dissolving of the underlying organic films. Finally, a 20 nm thick gold gate electrode was deposited by shadow-mask evaporation. Layer thicknesses were determined by a stylus profiler (DektakXT, Bruker).

Electrical characterisation of all devices was performed under nitrogen with an Agilent 4155B Semiconductor Parameter Analyser. Hole mobility values μ_h (cm²/Vs) were extracted from a linear fit of the transfer characteristics in the saturation regime using the following equation:

$$\mu = \left(\frac{\partial (I_D)^{1/2}}{\partial V_G} \right)^2 \frac{2L}{WC_{ox}}$$

where I_D is the source-drain current [A], V_G the gate voltage [V], W and L are the channel width and length [m], respectively, and C_{ox} [F/m²] is the dielectric layer capacitance per area unit. The intercept of the linear fit with the gate voltage axis gave V_{th} .

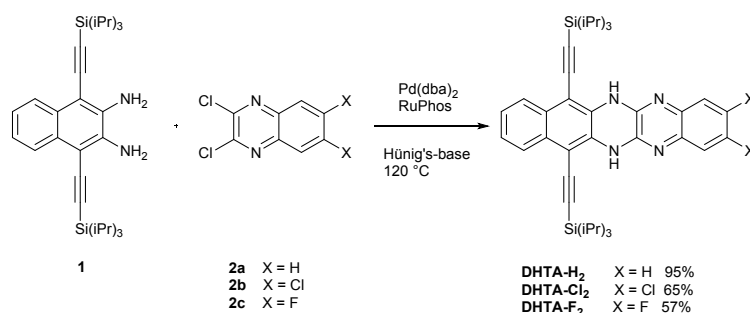
The characteristic device parameters were averaged from several batches of similarly performing devices with varying channel lengths and dielectric thicknesses.

X-Ray diffraction (XRD) on thin films: X-ray diffraction patterns of the films were recorded at 300 K using a Philips (now Panalytical) X'Pert diffractometer equipped with a Ge Johannson-type incident beam monochromator selecting the $K\alpha_1$ component of the Cu radiation generated in a corresponding X-ray tube ($\lambda = 1.54056 \text{ \AA}$). The diffractometer worked in Bragg-Brentano geometry, keeping the diffraction vector parallel to the film normal, whereby during the measurement the specimen was rotated around its normal. The horizontal and the axial divergence of the diffractometer ensured that also lattice planes with normals rotated by up to about 1° away from the specimen normal contribute to the diffraction pattern. In order to obtain precise values of d_0 from the diffraction data, one has to recognise that the reflection positions can be affected, in particular, at very low diffraction angles, by specimen displacement away from the focal circle of the diffractometer. Thereby, a reflection occurring at a diffraction angle of 2θ is shifted by (in radians) $\Delta 2\theta = -2s\cos\theta/R$ with R being the distance between specimen and diffractometer aperture and with s being the displacement of the specimen outward of the focussing circle. These height errors arose here to some extent because it was avoided to touch the specimen surfaces upon mounting the glass plates for the measurement onto some modelling clay. For evaluating the value of d_0 and to correct for the height error, pseudo-Voigt functions were fitted to all Bragg reflections belonging to the mentioned series or higher-order reflections. Using a starting value of d_0 and for the height error, both values were refined upon minimising the sum of squared differences between the observed diffraction angles and the diffraction angles calculated from d_0 , the reflection order n and for the displacement error s. Upon getting displacement errors of the order of $\pm 0.15 \text{ mm}$ the values of d_0 were obtained, which have been compiled in Table-S2. Note that in the case of the diffraction data **DHTA-F₂** two distinct values of d_0 were obtained (see above).

Single Crystal structure analysis was accomplished on Bruker Smart CCD, Bruker APEX and Bruker APEX II diffractometers. Single Crystals were grown either in solution from hexane/toluene mixtures or as described by drop-casting on polycrystalline films on polyimide. All crystals were free of solvent molecules.

B) Synthesis

Pd-catalyzed reaction of the diamine **1** with the dichloroquinoxalines **2a-c** furnished the targets **DHTA-X₂** in excellent yields between 57 and 95 %. The reaction is executed in the presence of the RuPhos ligand, most effective for these transformations.^{3,4} As solvent and as auxiliary base we employed Hünig's base. For **DHTA-Cl₂** and **DHTA-F₂**, the halides are not active enough to allow a second coupling, only the activated chlorides at the pyrazine ring react. The synthesised compounds are crystalline and purified by sequential chromatography and double crystallisation from pentane and from dichloromethane.



Scheme S1: Buchwald-Hartwig amination of **1** with **2a-c** to obtain dihydrotetraazaacenes **DHTA-X₂**.

Synthesis of *N,N'*-dihydrotetraazapentacenes **DHTA-H₂** and **DHTA-Cl₂** followed the procedure described by Tverskoy *et al.*³

*2,3-Difluoro-7,12-bis{tri(propan-2-yl)silyl}ethynyl}-6,13-dihydrobenzo[g]quinoxalino [2,3-b]quinoxaline (**DHTA-F₂**):*

Hünig's base (4 mL) was placed under Argon atmosphere in a dried Schlenk tube that contained **1** (400 mg, 771 μmol), 2,3-dichloro-6,7-difluoro-quinoxaline **2c** (270 mg, 1.16 mmol), RuPhos (18.0 mg, 5 mol %) and Pd(dba)₂ (22.2 mg, 5 mol %). The tube was sealed and the reaction mixture was stirred for 20 h at 100 °C. The reaction mixture was diluted with

methylene chloride and saturated aqueous NH_4Cl solution. After extraction of the aqueous phase with methylene chloride the organic phases were collected, dried over Na_2SO_4 and filtered through a pad of silica gel. After evaporation of the solvent the crude product was purified by flash column chromatography as yellow solid (silica gel, petroleum ether \rightarrow petroleum ether/methylene chloride 4:1, 299 mg, 57 %).

C) Analytical Data DHTA-F2

Melting point 261 °C; $^1\text{H-NMR}$ (400 MHz, CDCl_3): δ = 1.20-1.31 (m, 42H), 7.20 (t, 2H, J = 9.6 Hz), 7.34-7.40 (m, 2H), 7.58 (brs, 2H), 7.93-7.98 (m, 2H); $^{19}\text{F-NMR}$ (282 MHz, CDCl_3): δ = -138.29 (s, 2F); $^{13}\text{C}\{^1\text{H}\}$ -NMR (101 MHz, CDCl_3): δ = 11.44, 18.99, 98.95, 102.50, 106.06, 112.68 (q), 125.39, 126.40, 129.63, 131.37, 136.11 (t), 141.04, 149.73 (dd); IR: ν = 3375, 2941, 2864, 2126, 1593, 1463, 1424, 1280, 1259, 1160, 1046, 993, 881, 772, 757, 679, 556; UV-VIS λ_{max} (hexane): 455 nm; HR ESI: m/z $[\text{M} + \text{H}]^+$ calcd. for $\text{C}_{40}\text{H}_{51}\text{F}_2\text{N}_4\text{Si}_2^+$: 681.36307, found: 681.36223; elemental analysis: calcd. $\text{C}_{40}\text{H}_{50}\text{F}_2\text{N}_4\text{Si}_2$: C 70.55, H 7.40, N 8.23, found: C 70.26, H 7.49, N 8.42.

D) Optical properties of DHTA-compounds

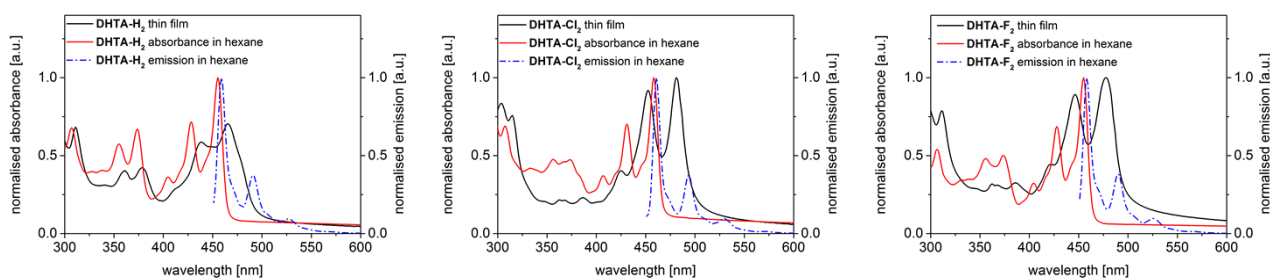


Fig. S1: Normalised absorbance (red) and emission (blue dotted) spectra of N,N' -dihydroetraazapentacenes in solution (hexane) and corresponding film (black) of **DHTA-H₂** (left), **DHTA-Cl₂** (middle) and **DHTA-F₂** (right).

Table S1: Optical parameters of **DHTA** obtained from UV-vis and fluorescence spectroscopies in hexane (excitation wavelength for emission spectra $\lambda = 450$ nm). Thin films were spin cast from toluene and annealed at 80 °C.

Compound	absorption sol. λ_{max} [nm]	emission sol. λ_{max} [nm]	stokes-shift [nm] ($[\text{cm}^{-1}]$)	absorption film λ_{max} [nm]	bathochromic shift λ_{max} film [nm]
DHTA-H₂	455	459	4 (192)	465	10
DHTA-Cl₂	458	461	3 (142)	481	23
DHTA-F₂	455	458	3 (144)	478	23

E) Polarised Optical Microscopy (POM)

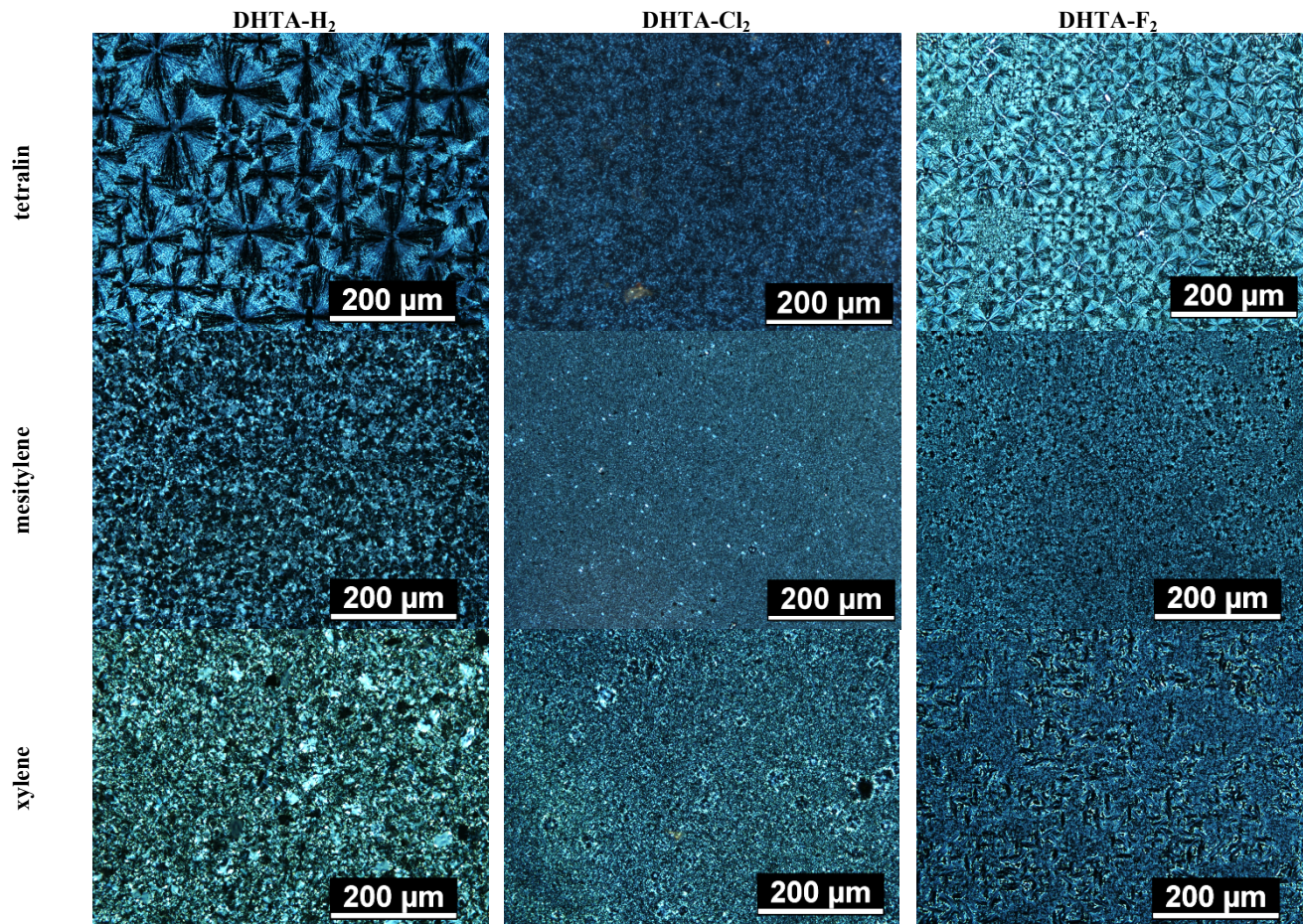


Fig. S2: Polarised optical microscopy images (crossed polarisers) of thin films of **DHTA-H₂** (left column), **DHTA-Cl₂** (middle column) and **DHTA-F₂** (right column), spin-cast on polyimide from different solvents tetralin (top row), mesitylene (middle row), and xylene (bottom row).

F) Electrical Characterisation

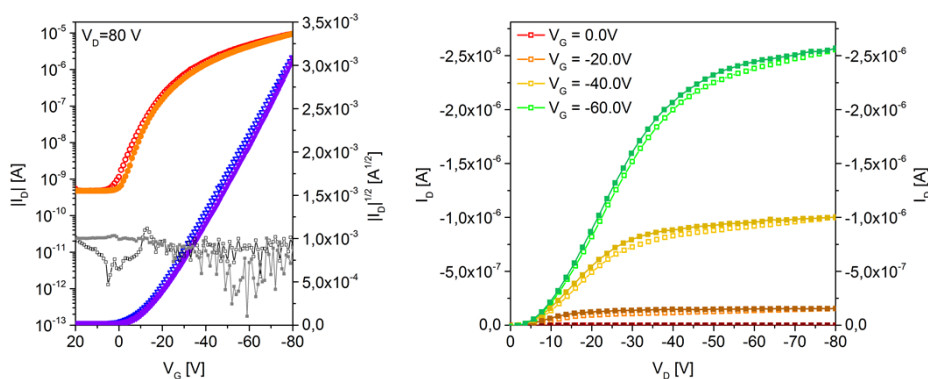


Fig. S3: Transfer of an average thin film transistor with **DHTA-H₂** as active layer (W/L = 1000 μ m / 20 μ m) at $V_{SD} = -80$ V (left) and output characteristic (right) spin-cast from tetralin.

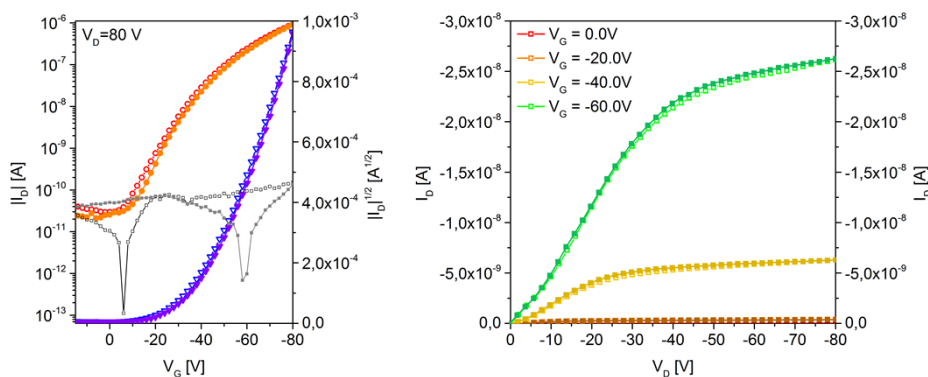


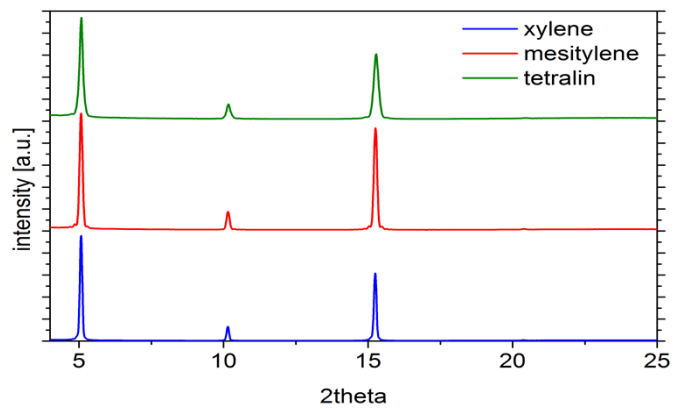
Fig. S4: Transfer of an average thin film transistor with **DHTA-F₂** as active layer (W/L = 1000 μ m / 20 μ m) at $V_{SD} = -80$ V (left) and output characteristic (right) spin-cast from mesitylene.

G) XRD data

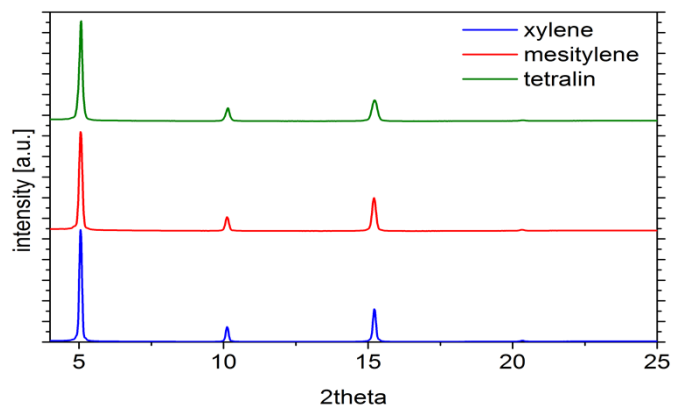
Table S2: Values of the fundamental lattice spacing d_0 pertaining to the series of higher order reflections from the films made from **DHTA-X₂** with xylene, mesitylene and tetralin as solvents.

molecule	d_0 (Å); solvent: xylene	d_0 (Å); solvent: mesitylene	d_0 (Å); solvent: tetralin
DHTA-H₂	17.42	17.41	17.38
DHTA-Cl₂	17.45	17.46	17.44
DHTA-F₂	18.02 and 17.39	18.02 and 17.36	17.99 and 17.38

DHTA-H₂



DHTA-Cl₂



DHTA-F₂

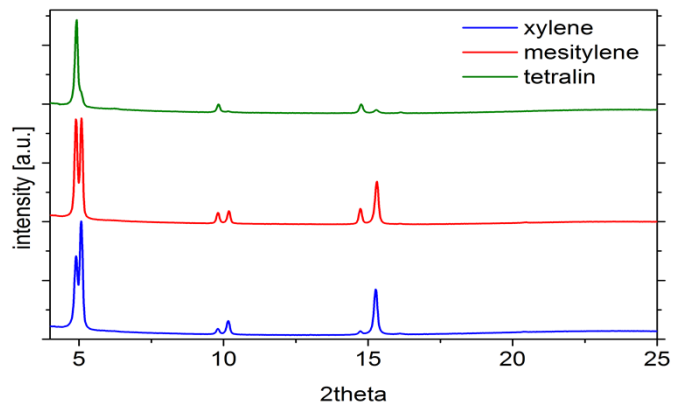


Fig. S5: X-ray diffraction pattern for DHTA-X₂ derivatives obtained from films on polyimide, spin-cast from different solvents recorded with Cu K α 1 radiation.

H) Summarised Structural data:

The crystal structures from solution grown crystals of **DHTA-H₂** and **DHTA-Cl₂** have been previously reported by Tverskoy *et al.*³. For more detailed information please use the .cif-files.

Single Crystal analysis for crystals grown from solution for **DHTA-H₂** (CCDC 803806):

“One-dimensional column-like packing”

$$a = 7.5919(18) \text{ \AA}, b = 13.551(3) \text{ \AA}, c = 18.320(4) \text{ \AA}, \alpha = 89.808(6)^\circ, \beta = 87.902(6)^\circ, \gamma = 81.114(6)^\circ$$

space group: $P\bar{1}$

For **DHTA-H₂** crystals grown on the polyimide substrate (drop-casting) the crystal parameters were determined to (CCDC 1021651)

“zig-zag pattern”

$$a = 7.7626(9) \text{ \AA}, b = 29.865(4) \text{ \AA}, c = 34.922(5), \alpha = 90^\circ, \beta = 95.412(3)^\circ, \gamma = 90^\circ$$

space group: $P2_1/n$

Single Crystal analysis for crystals grown from solution for **DHTA-Cl₂** (CCDC 803808):

“Paired herringbone pattern”

$$a = 14.8777(2) \text{ \AA}, b = 19.1070(1) \text{ \AA}, c = 14.2470(2) \text{ \AA}, \alpha = 90^\circ, \beta = 98.460(1)^\circ, \gamma = 90^\circ$$

space group: $P2_1/c$

Single Crystal analysis for crystals grown from solution for **DHTA-F₂** (CCDC 1021650)

“Brickwall packing of dimers”

$$a = 18.845(2) \text{ \AA}, b = 13.5519(13) \text{ \AA}, c = 16.4737(18) \text{ \AA}, \alpha = 90^\circ, \beta = 107.673(3)^\circ, \gamma = 90^\circ$$

space group: $P2_1/c$

At -73 °C another polymorphous phase was found for **DHTA-F₂** (CCDC 1021652)

“Slightly tilted Brickwall packing of dimers”

$$a = 16.4266(17) \text{ \AA}, b = 39.893(4) \text{ \AA}, c = 36.045(4) \text{ \AA}, \alpha = 90^\circ, \beta = 99.223(3)^\circ, \gamma = 90^\circ$$

space group: $P2_1/c$

I) References

1. H. E. Gottlieb, V. Kotlyar, and A. Nudelman, *J. Org. Chem.*, 1997, **62**, 7512–7515.
2. T. Sakanoue and H. Siringhaus, *Nat. Mater.*, 2010, **9**, 736–40.
3. O. Tverskoy, F. Rominger, A. Peters, H.-J. Himmel, and U. H. F. Bunz, *Angew. Chem. Int. Ed. Engl.*, 2011, **50**, 3557–60.
4. D. S. Surry and S. L. Buchwald, *Angew. Chem. Int. Ed. Engl.*, 2008, **47**, 6338–61.